Int. J. Environ. Res., 9(1):9-18,Winter 2015
ISSN: 1735-6865

Assessing the Value of Urban Green Spaces in Mitigating Multi-Seasonal Urban Heat using MODIS Land Surface Temperature (LST) and Landsat 8 data

Odindi, J. O.*, Bangamwabo, V. and Mutanga, O.

School of Agricultural, Earth and Environmental Sciences, University of KwaZulu-Natal, P. Bag X01, Scottsville, 3209 Pietermaritzburg, South Africa

Received 20 March 2014; Revised 4 July 2014; Accepted 18 Oct. 2014

ABSTRACT: Urban growth and associated landscape transformation has been a major driver of local, regional and global environmental change. The conversion of urban greenery to impervious landscapes has been identified as a key factor influencing the distinctive urban heat and associated consequences. Due to the often high demand for space in urban areas, creation and preservation of urban greenery as heat sinks is commonly perceived as "a waste of space". Consequently, there is an increasing need for creation and preservation of such spaces. This study sought to quantify multi-seasonal heat contribution of major Land-Use-Land-Cover (LULC) within the Ethekwini Municipal Area (EMA) using the recently launched Landsat 8 and MODIS - Land Surface and Temperature (LST) data-sets. To determine the contribution of urban greenery as possible remedy to Urban Heat Island (UHI), major LULCs were grouped into four functional zones and Contribution Index (CI) used to determine multi-seasonal heat contribution to EMA. Results show that impervious surfaces were the major heat source while the green spaces were the major heat sinks. Furthermore, the built-up/green spaces transition zones accounted for significantly lower heat contribution to the entire landscape. The latter finding indicates the value of developing greenery mosaics within the often densely built-up urban areas. In addition to determining extents of EMA's valuable greenery, this study demonstrates the value of remotely sensed data-sets in understanding the implication of LULC types on the urban micro-climate. The study is particularly valuable for designing sustainable urban socio-economic and environmental strategies at local, regional and global climate change

Key words: Urbanization, MODIS, Landsat, Green spaces, Remote Sensing, Urban Heat Island

INTRODUCTION

Sustained urban population influx and consequent transformation to impervious surfaces commonly result in a rural/urban ecological and climatic imbalance. Typically, urban growth involves replacement of natural vegetation with non-transpiring and non-evaporating impervious surfaces. Under clear solar heating, the impervious surfaces absorb and accumulate more solar radiation and impedes long-wave sky radiation loss (Rizwan *et al.*, 2008; Oke, 1988). The rough urban landscape inhibits wind movement and hence lowers convective heat loss while the reduced thermal inertia and vegetation index constrain heat loss from latent heat flux (Christen and Voogt, 2004). Furthermore, air pollutants influenced by urban waste heat lead to a built-up/natural landscape temperature contrast (Kondoh and Nishiyama, 2000; Weng, 2001). These factors induce the development of an urban heat island (UHI) (Oke, 1988). Generally, the rural/urban temperature difference in small towns is often modest (below 1°C); however, in bigger cities this difference may differ significantly (Mather, 1986).

Microclimatic conditions within the urban landscapes affect the comfort and health of urban residents, energy consumption and air quality (Huang *et al.*, 2008; Shahmohamadi, 2011; Hardy, 2003). Furthermore, UHI affects local weather by changing wind patterns, inducing formation of cloud and fog, increasing humidity and altering precipitation rates and cycles (Taha, 1999). Recent concerns on climate change and associated challenges have also been attributed to UHI.

Elevation of urban heat has been associated with a decline in urban green spaces (Tong *et al.*, 2005; Ca *et al.*, 1998; Ashie *et al.*, 1999; Yu and Hien, 2006; Kikegawa *et al.*, 2006; Spronken-Smith *et al.*, 2000).

*Corresponding author E-mail:Odindi@ukzn.ac.za

According to Kondoh and Nishiyama (2000), the loss of urban green vegetation leads to a reduction in heat loss from latent heat flux. Whereas UHI can be mitigated using multiple approaches, a number of studies (Rizwan *et al*., 2008; Tong *et al*., 2005; Ca *et al*., 1998; Ashie *et al*., 1999; Yu and Hien, 2006 and Spronken-Smith *et al*., 2000; Weng *et al*., 2003) note that creation and conservation of urban greenery is the most promising mitigation measure.

The severity of the intensity of urban heat depends on a city's location and characteristics (Parham *et al*., 2010). Typically, individual characteristics include size and density of population, level of industrialization, seasonality of the climate, and traffic pattern and density. Consequently, urban surface heat fluxes vary spatially within and between cities. Despite previous efforts made by many researchers, studies on UHI have been limited to only a few areas (Jin *et al*., 2005). Consequently, due to complex interaction of factors earlier mentioned and the uniqueness of each urban area, extrapolation of findings based on a limited number of cities to a global scale may not be valid. In this regard, understanding and quantification of place specific relationships between UHI and green spaces as possible heat remedy is critical in justifying the creation and maintenance of urban greenery. The quantification of such a relationship is particularly critical to a better understanding of urban bio-physical characteristics and processes which is necessary for sustainable socio-economic and environmental decisions.

Previously, Arnfield (2003) notes that studies on UHI have focused on single season analysis due to lack of multi-temporal data. However, multi-seasonal monitoring of urban heat remains a relevant requisite to understanding the implication of Land-Use-Land-Cover (LULC) types to year-long urban heat and energy balance. Traditionally, UHI studies have relied heavily on Land Surface and Temperature (LST) data from among others World Meteorological Organization (WMO) weather stations, in situ measurements, numerical models and small scale physical models (Rizwan *et al*., 2008; Voogt and Oke, 2003). However, changes in sites and instruments, inconsistent coverage of weather station data and challenges in validating numerical and spatial scale models limit the use of data from such sources (Peterson, 2003; Arnfield, 2003). In the recent past, consistency and wide scale spatial coverage has made satellite based remotely sensed datasets in concert with Geographical Information Systems (GIS) valuable in urban physical and bio-climatic studies. According to Rogan and Chen (2004), the value of remotely sensed datasets has further been driven by advances in sensor technology and therefore better data quality and the emergence of standardized processing methods. Furthermore, recent proliferation of remote sensing GIS software and algorithms have made it possible to reliably determine different physical and bio-climatic variables (Johnson, 2009).

Remotely sensed datasets are ideal for measurement of local, regional and global surface radiation (Dash *et al*. 2002). Commonly, NOAA's Advanced Very High Resolution Radiometer (AVHRR), Landsat's Thamatic Mapper (TM) and Enhanced Thematic Mapper (ETM) and Advanced Spaceborne Thermal Emission and Reflection Radiometer (ASTER) have been used in UHI studies (Gallo and Owen, 1998; Streutker, 2002; Weng, 2001; Nicol and Wong, 2005). However, in this study, we preferred MODIS dataset due to its high temporal resolution (twice daily) and therefore large data abundance at moderate spatial resolution.

The MODIS sensor is a critical instrument aboard National Aeronautics and Space Administration's (NASA's) *Terra* (EOS AM) and *Aqua* (EOS PM) satellites. Launched on 18th Dec 1999, MODIS – *Terra's* seven solar and three thermal spectral bands measure surface radiation at 10:30 and 22:30 ascending and descending local times respectively (Jin and Dickson, 2000). The MODIS - *Terra* determines the earth surface's skin temperature (T_{skin}) based on split window algorithm from thermal and mid-infrared bands at 1–km resolution at nadir. The values are corrected for atmospheric and surface effects to approximately 1 K root mean square error (Wan *et al*., 2004). Cloud-free values quality flags emissivity is then converted to broadband values using Moderate resolution transmittance (MODTRAN) (Jin *et al*., 2005).

To minimize the influence of cloud noise, we used the best quality cloud-free 1 km 8-day LST/emissivity (MOD11A2) imagery available. According to Wan and Dozier (1996), the LST data is based on bands 3-7, 13 and 16-19 for landscape emissivity, 26 for cloud detection and 20, 22, 23, 29, 31 and 32 for correction for atmospheric temperature and water vapour. The 8 day LST/emissivity is generated from clear sky daily (day/night) average based on thermal bands, atmospheric temperature and water vapour (Wan, 2006).

The Landsat 8, launched on 11/02/2013, is the latest of the Landsat series. It is characterized by 11, 30m multispectral bands and a 15m panchromatic band. The Landsat imagery series has the longest history in LULC mapping. Consequently, their reliability in LULC mapping is widely reported in literature. In this study we use multi-seasonal MODIS-LST in concert with Landsat–8 Operational Land Imager (OLI) data to

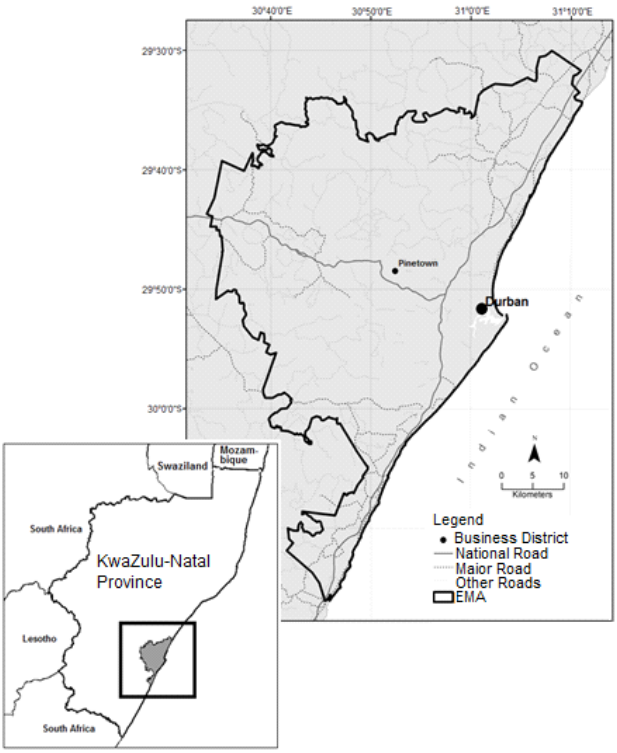

Fig. 1. The study area

quantify heat contribution from different functional zones in the four seasons. The study further sought to establish the potential of urban greenery as possible mitigate to urban heat elevation.

The study was conducted in the Ethekwini Municipal Area (EMA), KwaZulu-Natal Province, South Africa (Fig. 1). The municipality is regarded as the second most important manufacturing area in the country. The EMA is made up of Durban, the third largest city in South Africa and adjacent smaller towns and accommodates 33% and 7% of the province and country's population respectively (EM IDP, 2013). Based on the 2011 population survey, the municipality has 3.5 million people and covers 2,292 km^2 at 1513 people/km^2 (SSA, 2012). According to the Ethekwini Municipality IDP (2013), EMA's central urban core in the Durban city is the most densely populated and accommodates 35% of the area's population.

The EMA is characterized by Humid Subtropical Climate (Köppen climate classification-*Cwa*) with hot and humid summers and mild dry winters. The altitude ranges from sea level to over 300m on the metro's fringes. Precipitation in the area varies considerably, from 500mm to over 2000 mm per annum. Typically, the area receives mean annual precipitation of 1,000mm. Summer (November-April) and winter (May-October) are wet and dry respectively (CAMP, 1997). Temperatures range between 20-35 °C and 12-25 °C in summer and winter respectively (Scott-Shaw *et al*., 1996). Prevailing winds blow parallel to the coast with south-westerly and north-easterly winds alternating with seasons (CAMP, 1997).

Due to urbanization, almost all the terrestrial habitat within the EMA has been substantially transformed (EM IDP, 2013). Furthermore, invasive plant species, pollution and climate change related impacts are regarded as major threats to the area's green environment. However, despite existing threats to the areas' habitat, portions of the EMA's greenery have been conserved through controlled development, environmental servitudes and land acquisition for conservation. Consequently, some areas have remain in near pristine conditions.

MATERIALS & METHODS

MODIS (MOD11A2) Version 5 from MODIS - *Terra* instrument was used in this study. The 8 day day/night LST 1 km imagery were acquired from the Land Process Data Archive Center (LPDAAC), Earth Resources Observation and Science (EROS) Center, U.S. Geological Survey. Two MODIS imagery scenes were required to cover the entire study area for each season, consequently, two adjacent images (Horizontal/vertical tile no 20/11 and 20/12) were used. Eight scenes closest to the four season's mid dates - (17-24/01/2012), (14-21/04/2012), (19-26/07/2012) and

(15-22/10/2012) for Summer, Autumn, Winter, Spring respectively were acquired, geo-rectified, resampled and clipped for analysis. The multi-seasonal LST data was then converted from Kelvin x 200 to degrees Celcius using the equation:

$$LST_R = \left(LST_I^* 0.02\right) - 237.15 \quad (1)$$

where: LST_R is the rescaled LST digital values and LST_I is the original image digital values (see Fig. 3).

A wide body of literature (Wan and Li, 2002; Wan *et al*., 2004; Coll *et al*., 2009; Wan and Li, 2008 among others) has established high reliability (<1 K accuracy) of MODIS LST on urbanized and natural landscapes with varying atmospheric conditions. Despite this high reliability, the MODIS LST was validated using temperature readings from the weather station at the area's major airport. In consistency with aforementioned literature, the differences between the airport's impervious surface temperature and MODIS LST data were less half a degree and therefore considered negligible.

A Landsat–8 Operational Land Imager (OLI) imagery (path/row-168/81) acquired on 24/06/2013 was used to determine LULC types. The Landsat image and a closest corresponding aerial photo (taken in mid-2012) were first rectified to Universal Transverse Mercator (UTM) projection and World Geodetic System 1984 (WGS84) datum. The image was then geo-rectified using common points identified in the 1:50 000 topographic maps, aerial photographs and well distributed GPS data acquired from the field. To determine the LULC classes, a hybrid classification technique comprising supervised and unsupervised classifications was adopted. The unsupervised classification technique was used to gain an insight into the number of major spectral differences in the image. This insight was then used as a basis to determine broad LULC using supervised classification. Maximum likelihood algorithm was then used to

Table 1. Major LULC classes and their respective Functional zones

Original LULC classes	Re-coded class	Functional zone
Indegenous forest, Plantations forest, Thicket, Water body, Wetland	Dense vegetation (including water bodies)	**Dense green space**
Cultivated land, Grassland, Mixed vegetation (Shrub/Grassland)	Low density vegetation	**Low/sparce green space**
Bare soil, Medium Density Residential, Low Density Residential, Roads, Bare soil/Cleared land, Quarry	Moderately built-up (including bare soil)	**Moderately built-up**
Built up (Commercial), Built up (Industrial), Dense (Residential)	Densely built-up	**Densely built-up**

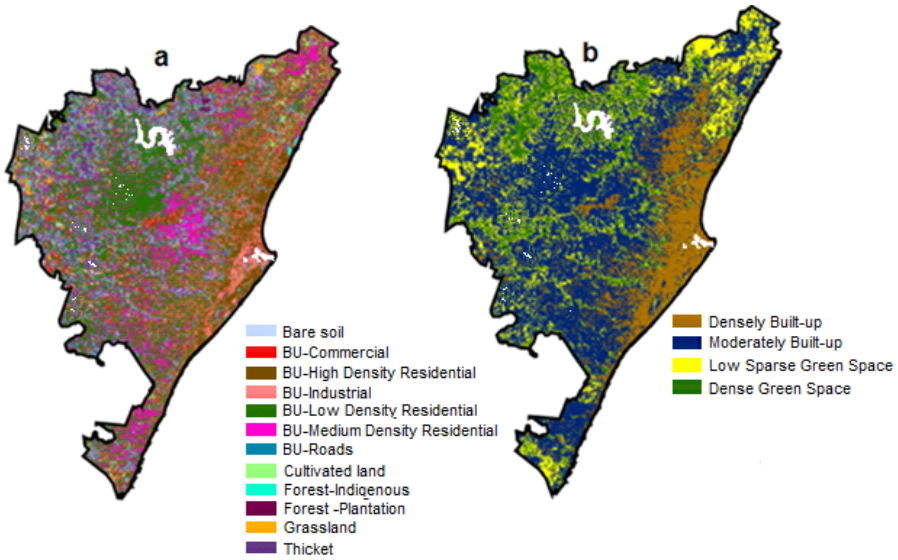

Fig. 2. Distribution of major LULC type and respective Functional zones, a-LULC classes and b-respective Functional zones - (BU-Built-up). White areas represent masked out water bodies and bare surfaces

amalgamate LULC classes into fewer related classes for assessing their heat contribution to the EMA (Table 1). During the classification process, two types of surfaces (water bodies and bare surfaces) that were neither impervious surfaces nor urban greenery were picked up. In consistency with literature (see; Weng, 2001; Chen *et al*., 2006; Yuan, 2007), a preliminary analysis indicated that the heat contribution by the two surfaces were similar to Dense green spaces and Moderately built-up areas respectively. However, since these areas can neither be categorized as green spaces nor built-up areas, they were masked out before analysis (Fig. 2). Due to a high multiplicity, similarity and limited extents of most of the EMAs LULCs, related LULC types were amalgamated into broad functional zones and labeled as Heavily built-up, Moderately built-up, Low/sparse green spaces and Dense green spaces respectively (Figs. 2 a and b). This process was also considered necessary in decreasing redundancy in the analysis. Post classification smoothing was done on the LULC and functional zone maps to remove noisy pixels. The classification accuracy was then assessed by comparing the LULC classes and corresponding covers identified on the aerial photographs and spatial data from field visits. In each case over 85% accuracy was achieved.

Using Formula 2 and 3, OLI's visible, near-infrared and short-wave infrared bands were used to compute Normalized Difference Vegetation Index (NDVI) and Normalized Difference Built Index (NDBI) respectively. Values from these indices were used to determine the correlation and levels of greenness and impervious surfaces. To verify the types of LULC classes occupied by results from the two indices outputs, the LULC were overlaid on the NDVI and NDBI. The results from the indices were then related to the LST data.

$$NDVI = (OLI_5 - OLI_4) / (OLI_5 + OLI_4) \quad (2)$$

$$NDBI = (OLI_7 - OLI_5) / (OLI_7 + OLI_5) \quad (3)$$

where: OLI_4 (0.630-0.680μm) is the red band, OLI_5 (0.845-0.885μm) is the near-infrared band and OLI_7 (1.560-1.660μm) is the second short-wave infrared band.

To determine the contribution of the area's green spaces in relation to other LULC types in mitigating UHI, over 5000 well distributed points were randomly extracted from each of the functional zones. These points were then used to extract corresponding LST values for the four seasons. In consideration of the possible varying seasonal temperature and atmospheric conditions during LST acquisition, the temperature means of functional zones in relation to the entire landscape for each of the seasons were computed separately. With the mean seasonal temperature for all the pixels within the study area as baseline, the seasonal thermal influence of each of the functional zones to the entire urban landscape was computed by the Contribution Index (*CI*) – (Chen *et al*., 2006) using function:

$$CI = D_t \times S \quad (4)$$

where: *CI* is the influence of the zone to the entire landscape, D_t is the difference in mean temperatures between the zone and the entire urban landscape, and *S* is the proportion of the area to the entire landscape.

RESULTS & DISCUSSION

The multi-seasonal LST data showed apparent spatio-temporal variability in land surface temperature (Fig. 3). The eastern and western parts of the EMA were characterized by higher and lower temperatures respectively (Fig. 3). The mid-eastern parts of the EMA (city of Durban) showed the highest temperature values while the eastern and southern parts of the EMA showed relatively lower temperatures in all the seasons (Fig. 3). Based on the LST values extracted from the MODIS multi-seasonal layers, maximum, mean and minimum temperatures were higher in summer than in winter (Fig. 4). The summer maximum, mean and minimum temperatures were 36.37, 30.30 and 24.23 ^{o}C respectively while winter maximum, mean and minimum were 24.27, 20.91 and 17.55 ^{o}C respectively. However, whereas there was no significant difference in the mean and minimum temperature values in autumn and spring, there was a significant difference in maximum values between the two seasons (Fig. 4).

There was a strong negative correlation between the green surfaces and built-up areas (Fig. 5). This correlation provides an indication that an increase in built-up areas leads to a decline in green spaces and vice versa. The Moderately built-up functional zone (Medium density residential, Low density residential, Roads) and the Densely built-up functional zone (Commercial, Industrial and Dense Residential) were the most dominant and the second most dominant landscapes respectively (Table 2). The Dense green space (Indigenous forest, Plantation forest, Thicket, Wetland) and the Low/sparse green space (Cultivated land, Grassland, Mixed vegetation) were the second smallest and smallest functional zones respectively. These areas constituted a proportion of 0.126 and 0.087 respectively (Table 2). The Densely built-up and the Dense green space functional zones had consistently high positive and high negative multi-seasonal deviations from the entire landscape's means. Deviations of 1.995 ^{o}C in summer and -1.07 ^{o}C during winter were the highest and lowest respectively (Table 3). Whereas the Densely built-up and Dense green

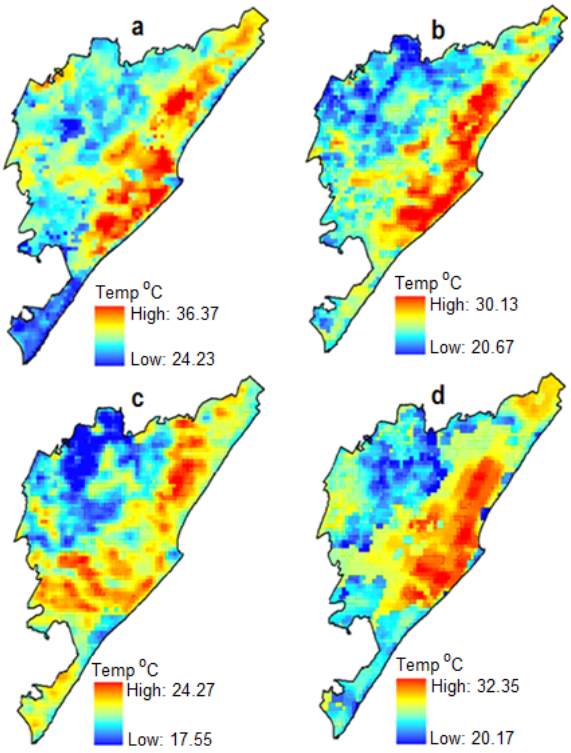

Fig. 3. Multi-seasonal temperature distribution within the EMA (a-summer, b-autumn, c-winter, d-spring)

space functional zones showed respective consistently high positive and high negative deviation from mean, the multi-seasonal patterns for the Moderately built-up and Low/sparse green space functional zones were not consistent (Table 3). For instance, Moderately built-up's temperature deviation was higher than Low/sparse green space in summer while the latter was higher in autumn (Table 3). A similar inconsistency was noted in winter and spring (Table 3). In summer, based on the amount of heat and total area, Densely built-up functional zone provided the most significant amount of heat to the EMA while the Dense green space functional zone provided the least amount of heat (Fig. 6). A similar trend was evident in the rest of the seasons. During summer, autumn and spring, the Low/sparse green space had a higher heat contribution than the Moderately built-up functional. However in spring, there was a higher contribution by the Moderately built-up functional zone than the Low/sparse green space. There was a near similar contribution of heat from the Densely built-up functional class in summer (0.501), autumn (0.469) and spring (0.478) while the winter functional zone's contribution was significantly lower (0.209). Generally, there was a gradual decrease in the amount of heat emitted by the Dense green space functional zone in summer, autumn, winter and spring months. The greatest heat contribution was by the Densely built-

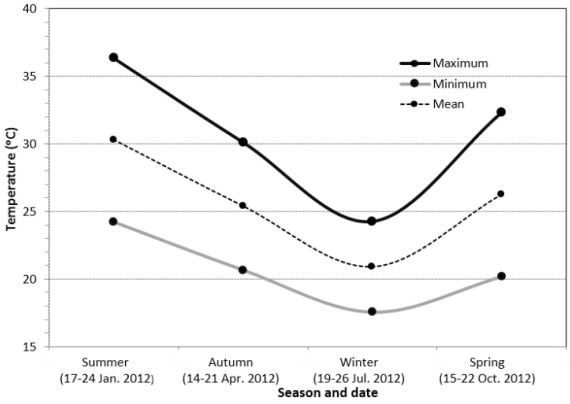

Fig. 4. Seasonal temperature values based on the area's MODIS LST pixels

up functional zone in summer while the least amount of heat was by the Dense green space functional zone in Spring (Fig. 6).

Annual heat contribution within the EMA was determined by computing the average temperature values for the EMA's dense greenery in relation to other cover types. In the four functional zones, only the Dense built-up areas had a positive contribution index (+0.414). Consequently, the Densely built-up functional zone can be considered as main heat source within the EMA. The Moderately built-up and Low/Sparse green space functional zones had marginally negative heat contribution within the study area (-0.045 and -0.053) and can therefore be considered to be of marginal value in mitigating urban heat. Based on this result, it can be assumed that the heat source/sink role in a built-up/vegetation mosaic is determined by their individual density. The Dense green space functional zone had the least annual heat contribution (-0.442). This functional zone can therefore be regarded as the most valuable heat sink within the EMA. Based on these annual heat contributions, spatial extents of the most valuable heat sinks within the EMA are presented. Urbanization and consequent LULC transformation have a direct effect on local bio-climatic conditions which in turn affect environmental quality. Mapping of urban LULC *vis-à-vis* urban micro-meteorological patterns is crucial to understanding and mitigating the impacts of urban LULCs on local, regional and global climate (Mahmood *et al*., 2010). According to Huang *et al*. (2008), studies on the relationship between UHI and urban LULC change and its impact on environmental quality are not limited to pursuit of more knowledge, but also practical needs of urban planning. Due to the limitations of traditional mapping techniques noted by Davey and Pielke (2005) and Pielke *et al*. (2007) among others, remotely sensed datasets sets have great potential in relating LST to different LULCs types. The spatial and temporal resolutions that characterize

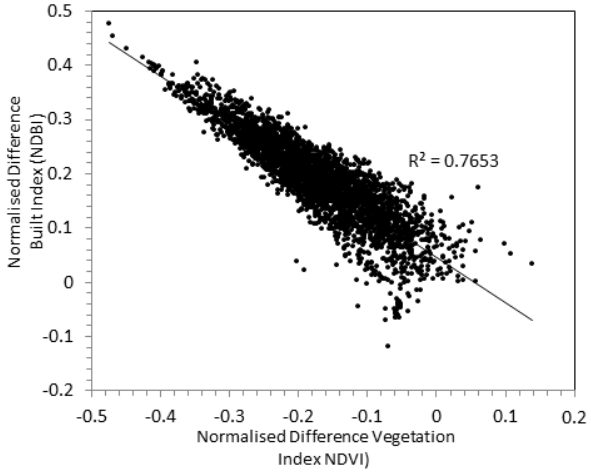

Fig. 5. Correlation between NDVI and NDBI

Table 2. Spatial extents and proportions of the functional zones

Functional Zone	Area (Ha)	Cover area (%)	Proportion
Densely built-up	57631.59	25.07	0.251
Moderately built-up	122913.27	53.62	0.536
Low/sparse green space	19705.77	8.67	0.087
Dense green space	28963.8	12.64	0.126
Total	229214.43	100	1

Table 3. Seasonal temperature deviations from respective means

Functional Zone	Season mean and functional zone deviation (°C)			
	Summer (30.02)	Autumn (25.22)	Winter (21.36)	Spring (26.61)
Densely built-up	1.995	1.87	0.83	1.903
Moderately built-up	-0.78	-0.53	-0.15	-0.72
Low/sparse green space	-0.76	-0.56	-0.23	-0.11
Dense green space	-0.83	-0.77	-0.92	-1.07

remotely sensed imagery are particularly valuable in correlating multi-temporal urban climatic variables and urban greenery simultaneously. Using MODIS LST and Landsat OLI datasets, this study established seasonal variation between the LULC types represented by the four functional zones within EMA. Respective heat generated by densely built-up/urban greenery areas for instance were 32.02/29.48 °C, 27.09/24.45 °C, 22.19/20.43 °C and 28.51/25.53 °C in summer, autumn, winter and spring, respectively. Whereas this study was conducted in the Southern Hemisphere's Humid Subtropical climate, and therefore different physical location to studies in existing literature, the findings are consistent with those from Shudo *et al*. 1997; Chudnovsky 2004 and Eliasson 1996 among others significant micro-scale temperature variation for major LULC types in cities of Goteborg, Hokkaido and Tel-Aviv in the northern hemisphere.

The LULCs associated with the Built-up functional zone had the highest multi-seasonal heat contribution to the EMA. According to Kjelgren and Montague (1997) and Oke (1982) such high contribution within the urban landscape can be attributed to thermal properties of impervious surfaces. These properties lead to greater short-wave absorption due to urban canyon geometry, reduction in net longwave loss, increased heat flux due to decrease in vegetation related evaporation and increased surface roughness which limits peripheral winds and hinders sensible heat loss (Oke, 1982). As expected, the contribution of Densely built-up areas was high in summer, autumn and spring (refer to Fig. 6). The heat contribution was however significantly lower in winter due to lower solar radiation. The Moderately built-up and the Low/sparse green space functional zone had a negative heat contribution in all the seasons (refer to Fig. 6). Apart from winter season, the Moderately built-up functional zone had a consistently lower negative heat contribution than the Low/sparse green space functional zone in all the seasons. Furthermore,

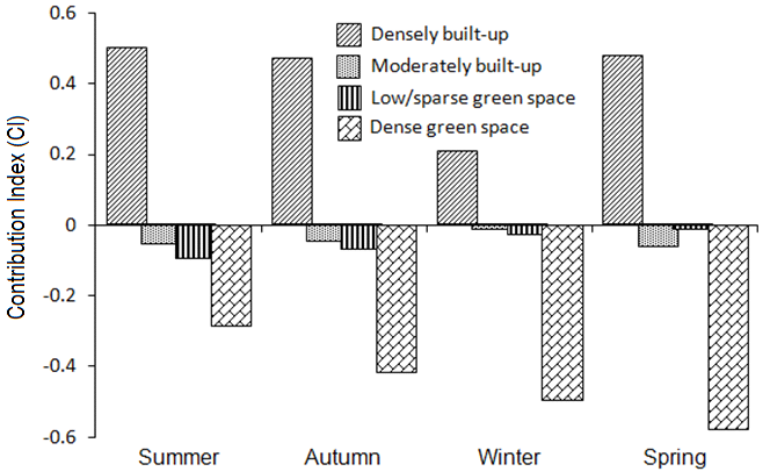

Fig. 6. Seasonal contribution of the different functional zones

there was a gradual decline in negative contribution of these surfaces in summer, autumn and winter respectively (refer to Fig. 6). These observations can be attributed to the peak summer rainfall season which leads to more vibrant Low/sparse vegetation and therefore more significant heat sinking. This vibrancy declines during the drier autumn and winter seasons and correspondingly the functional zones heat sink ability (refer to Fig. 6). In spring, the peak effect of drought on vegetation during autumn and winter reduce the functional zones ability as a heat sink to its lowest.

As aforementioned, Built-up functional zone showed consistently high multi-seasonal heat contribution. Consequently, these findings suggest that urbanization has the greatest contribution to localized temperature elevation with potentially high contribution to global warming. Conversely, LULC types grouped under the Green space functional zone had significantly low multi-seasonal heat contribution. This finding follows the built-up heat source and vegetation heat sink that characterize most urban landscapes. In this regard, as suggested by a number of authors (Tong *et al*., 2005; Ca *et al*., 1998; Ashie *et al*., 1999 and Yu and Hien, 2006 among others), consideration of urban heat sinks is critical in designing sustainable urban plans. Such initiatives could off-set the local high urban temperature and mitigate global warming (Chen *et al*., 2006).

Whereas a number of measures can be adopted to mitigate urban heat and its effects, Kikegawa *et al*. (2006) and Ashie *et al*. (1999) note that increase of urban greenery is the most feasible. In this study, the Dense green space functional zone was characterized by a gradual increase in negative heat contribution in summer, autumn, winter and spring respectively (Fig. 6). The increased autumn's negative contribution can be attributed to dense vegetation's slow response after peak summer rain while winter and spring's high negative contribution can be attributed to a combination of the dense vegetation vigour from summer rain, the low winter temperatures and low radiative winter temperature inertia. In consistency with other studies like Owen *et al*. (1998), Gallo and Owen (1998) and Weng (2001), the characteristic dense greenery of this functional zone can therefore be regarded as the most valuable heat sink within the EMA. In a related study by Sponken-Smith *et al*. (1999), green spaces could reduce urban temperatures by as much as 300% in comparison to the densely built-up surrounding, while Akbari *et al*. (1992) note that trees and urban parks decrease local air temperature by 0.5-5^{o}C. According to Konopacki and Akbhari (2002), the adoption of such mitigation measures could reduce carbon emission by 170000 tones in a city like Houston while Rosenfeld *et al*. (1998) notes that an ozone level of over 240 ppbv could be reduced to 120 ppbv by reducing urban temperature from 32^{o}C to 20^{o}C.

Whereas results in this study show that MODIS LST data can be valuable in establishing the heat contribution of fairly large and homogeneous LULCs to the urban landscape, the moderate MODIS LST spatial resolution (1km) may not accurately determine the value of smaller urban green spaces like open public parks and roadside and residential vegetation. In such landscapes, use of higher spatial resolution sensors like Landsat imagery are more suitable. Although efficacy of such small heat sinks can be compromised by net heat advection caused by humidity, wind and the dense impervious surfaces around them (Rizwan *et al*. 2008), Weng *et al*. (2003) note that such open spaces remain critical in mitigating short-term urban heat and long-term climate change.

CONCLUSIONS

In the recent past, remotely sensed datasets have emerged as valuable datasets in landscape analysis. Using the contribution index (CI) on multi-seasonal MODIS LST and the recently launched temporal Landsat 8 datasets, this study has demonstrated the value of remotely sensed data in understanding the influence of urban LULC types on LST. The qualitative and quantitative evidence from remotely sensed data can be valuable is designing current and future sustainable urban socio-economic and environmental plans. The consistently high negative CI in areas covered by vegetation is a clear indication of the value of the urban green landscape in mitigating UHI. Furthermore, this study shows that an integration of built-up and urban greenery is a valuable measure in mitigating urban heat. Consequently, initiatives like greening of suburbs and industrial zones are valuable measures in mitigating urban heat. This study concludes that the creation and maintenance of urban greens is a critical measure in sustainable urban planning. Such measures are therefore critical in mitigating global warming and climate change and associated implications.

ACKNOWLEDGEMENTS

We would like to thank the Earth Resources Observation and Science (EROS) - U.S. Geological Survey and the Land Remote Sensing Program of the U.S. Geological Survey in collaboration with NASA for generously availing the MODIS LST and Landsat 8 data.

REFERENCES

Akbari, H., Davis, S., Dorsano, S., Huang, J. and Winnett, S. (1992). Cooling our communities-A guidebook on tree planting and light coloured surfacing. US Environmental Protection Agency. Pittsburgh, Pennsylvania; Office of Policy Analysis, Climate Change Division.

Arnfield, A. (2003). Two decades of urban climate research: a review of turbulence, exchanges of energy and water, and the urban heat island. International Journal of Climatology, **23**, 1-26.

Ashie, Y., Thanh, V. and Asaeda, T. (1999). Building canopy model for the analysis of urban climate. Journal of Wind Engineering and Industrial Aerodynamics, **81**, 237-248.

Ca, V. T., Asaeda, T. and Abu, E. M. (1998). Reductions in air-conditioning energy caused by a nearby park. Energy and Buildings, **29**, 83-92.

CAMP, (1997). The Bioresource Groups of KwaZulu-Natal. Cedara Report, Pietermaritzburg, South Africa.

Chen, X., Zhao, H., Li, P. and Yin, Z. (2006). Remote sensing image based analysis of the relationship between urban heat island and land use/cover changes. Remote Sensing of Environment, **104**, 133-146.

Christen, A. and Voogt, R. (2004). Energy radiation balance of a central European city. International Journal of Climatology, **24**, 1395-1421.

Chudnovsky, A., Ben-Dor, E. and Saaroni, H, (2004). Diurnal thermal behavior of selected urban objects using remote sensing measurements. Energy and Buildings, **36**, 1063-1074.

Coll, C., Caselles, V., Valve, J. M., Valor, E., Niclos, R., Sanchez, J. M. and Rivas, R. (2005). Ground measurements for the validation of land surface temperatures derived from AATSR and MODIS data. Remote Sensing of Environment, **97,** 288-300.

Coll, C., Wan, Z. and Galve, J. M. (2009). Temperature-based and radiance-based validations of the V5 MODIS land surface temperature product. Journal of Geophysical Research, **114 D20 27**, 1-15.

Dash, P., Göttsche, F. M., Olesen, F. S. and Fischer, H. (2002). Land surface temperature and emissivity estimation from passive sensor data: Theory and practice-current trends. International Journal of Remote Sensing, **23**, 2563-2594.

Davey, C. A. and Pielke, R. A. (2005). Microclimate exposures of surface based weather station-implications for assessment of long-term temperature trends. Bulletin of the American Meteorological Society, **86**, 497-504.

Eliasson, I. (1996). Urban nocturnal temperatures, street geometry and land use. Atmospheric Environment, **30**, 379-392.

EM IDP, (2012). Ethekwini Municipality Integrated Development Plan, 2012/13 to 2016/17. Durban, Ethekwini Metro.

Gallo, K. P. and Owen, T. W. (1998). Assesment of urban heat island: a multi-sensor perspective for the Dallas –Ft, Worth, USA Region. Geocarto International, **13,** 35-41.

Hardy, J. T. (2003). Climate change: causes, effects and solutions. London: John Wiley.

Huang, L., Li, J., Zhao, D. and Zhu, J. (2008). A field study on the diurnal changes of urban microclimate in four types of ground cover and urban heat island of Nianjing, China. Building and Environment**, 43**, 7-17.

Jin, E. T. and Dickson, R. E. (2000). A Generalized algorithm for retrieving cloud sky skin temperature from satellite thermal infrared radiances. Journal of Geophysical Research, **D22**, 37-47.

Jin, M., Dickson, R. E. and Zhang, D. (2005). The footprint of urban areas on global climate as characterized by MODIS. Journal of Climate, **18**, 1551-1565.

Johnson, S. J. (2009). An evaluation of land change modeler for ARCGIS For the ecological

analysis of landscape composition. PhD Dissertation, Southern Illinois University.

Kikegawa, Y., Genchi, Y., Yoshikado, H., Kondo, H. and Hanaki, K. (2006). Impacts of city-block-scale counter measures against urban heat island phenomena upon building's energy consumption for air conditioning. Applied Energy, **83,** 649-668.

Kjelgren, R. and Montague, T. (1997). Urban tree transpiration over turf and asphalt surfaces. Atmospheric Environment, **32**, 35-41.

Kondoh, A. and Nishiyama, J. (2000). Changes in hydrological cycle due to urbanization in the suburb Tokyo Metropolitan area, Japan. Advances in Space Research, **26**, 1173-1176.

Konopacki, S. and Akbari, H. (2002) Energy savings for heat island reduction strategies in Chicago and Houston (including updates for Baton Rouge, Sacramento and Salt Lake City). Draft Final Report, LBNL – 49638, University of Califonia, Berkeley.

Mahmood, R., Pielke, R., Hubbard, K. G., Niyogi, D. and Bonan, G. (2010). Impacts of land use/land cover change on climate and future research priorities. Bulletin of the American Meteorological Society, **91**, 37-45.

Mather, A. S. (1986). Land use. London: Longman). pp. 286.

Nicol, J. and Wong, M. S. (2005). Modelling urban environmental quality in a tropical city. Landscape and Urban Planning, **73**, 49-58.

Oke, T. R. (1988). The urban energy balance. Progress in Physical Geography, **12**, 471-508.

Oke, T. R. (1982). The energetic basis of the urban heat island. Quarterly Journal of the Royal Meteorological Society, **108**, 1-24.

Owen, T. W., Carlson, T. N. and Gillies, R. R. (1998). An assessment of satellite remotely-sensed land cover parameters in quantitaivey describing the climatic effect of urbanization. International Journal of Remote Sensing, **19**, 1663-1681.

Parham, A. M. and Haghighat, F. (2010). Approaches to study Urban Heat Island – abilities and limitations. Building and Environment, **45**, 2192-2201.

Peterson, T. C. (2003). Assessment of urban versus rural in situ surface temperatures in the contiguous United States: No difference found. Journal of Climate, **16**, 2941-2959.

Pielke, R. A., Nielsen-Gammon, J., Davey, C., Angel, J., Bliss, O., Doesken, N., Cai, M., Fall, S., Niyogi, D., Gallo, K., Hale, R., Hubbard, K., Lin, X., Li, H., and Raman, S. (2007). Documentation of uncertainties and biases associated with surface temperature measurements sites for climate change assessment. Bulletin of the American Meteorological Society, **88**, 913-928.

Rizwan, A. M., Dennis, Y. C. and Liu, C. (2008). A review on the generation, determination and mitigation of urban heat island. Journal of Environmental Sciences, **20**, 120-128.

Rogan, J. and Chen, D. M. (2004). Remote sensing technology for mapping and monitoring

land-cover and land-use change. Progress in Planning, **61**, 301-325.

Rosenfeld, A. H., Akbari, H. and Romm, J. J. (1998). Cool communities: Strategies for heat island mitigation and smog reduction. Energy and Buildings, **28**, 51-62.

Scott-Shaw, C. R., Bourrouin, O. and Porter, R. N. (1996). The conservation status of Acocks' veld types in KwaZulu-Natal. Lammergeyer, **44**, 50-63.

Shahmohamadi, P., Che-Ani, A. I., Etessam, I., Maulud, K. N. A. and Tawil, N. M. (2011). Healthy environment: the need to mitigate urban heat island effect on human health. Procedia Engineering, **20**, 61-70.

Shudo, H., Sugiyama, J., Noriyoshi, Y. and Oka, T. (1997). A study of temperature distribution influenced by various land uses. Energy and Buildings, **26,** 199-205.

Spronken-Smith, R. A., Oke, T. R. and Lowry, W. P. (2000). Advection and surface energy balance across an irrigated urban park. International Journal of Climatology, **20**, 1033-1047.

SSA, (2012). Statistics South Africa, General household survey, 2011. (Statistics South Africa: Pretoria).

Streutker, D. R. (2002). A remote sensing study of the urban heat island of Houston, Texas. International Journal of Remote Sensing, **23**, 2595-2608.

Taha, H. (1999). Modifying a mesoscale meteorological model to better incorporate urban heat storage: a bulk-parameterization approach. Journal of Applied Meteorology, **38**, 466-473.

Tong, H., Walton, A., Sang, J. and Chan, J. C. (2005). Numerical simulation of urban boundary layer over complex terrain of Hong Kong. Atmospheric Environment, **39**, 3549-3563.

Voogt, J. A. and Oke, T. R. (2003). Thermal remote sensing of urban climates. Remote Sensing of Environment, **86**, 370-384.

Wan, Z. (2004). MODIS land surface temperature group. Retrieved from http://www.icess.ucsb.edu/modis on15-9-2013.

Wan, Z. (2008). New refinements and validation of the MODIS land-surface temperature/emissivity products. Remote Sensing of Environment, **112**, 59-74.

Wan, Z. and Dozier, J. (1996). A generalized split-window algorithm for retrieving land-surface temperature from space. IEEE Transactions on Geoscience and Remote Sensing, **34**, 892-905.

Wan, Z. and Li, Z. L. (2008). Radiance-based validation of the V5 MODIS land-surface temperature product. International Journal of Remote Sensing, **29**, 5373-5395.

Wan, Z., Zhang, Y. L., Zhang, Q. C. and Li, Z. L. (2004) Quality assessment and validation of MODIS global land surface temperature. International Journal of Remote Sensing, **25**, 261-274.

Weng, Q. (2001). A remotes sensing –GIS evaluation of urban expansion and its impact on surface temperature in Zhujiang Delta, China. International Journal of Remote Sensing, **22**, 1999-2014.

Weng, Q., Lu, D. and Schubring, J. (2003). Estimation of land surface temperature-vegetation abundance relationship for urban heat island studies. Remote Sensing of Environment, **89**, 467-483.

Yuan, F. and Bauer, M. E. (2007). Comparison of impervious surface area and normalized difference vegetation index as indicators of surface urban heat island effects in Landsat imagery. Remote Sensing of Environment, **106,** 375-386.

Yu, C. and Hien, W. N. (2006). Thermal benefits of city parks. Energy and Buildings, **38**, 105-120.